Int. J. Heat Mass Transfer. Vol. 35, No. 1, pp. 101–109, 1992
Printed in Great Britain

0017–9310/92 $5.00 + 0.00
© 1991 Pergamon Press plc

Prediction of heat transfer by direct contact condensation at a steam–subcooled water interface

AKIRA MURATA, EIJI HIHARA and TAKAMOTO SAITO
Department of Mechanical Engineering, The University of Tokyo,
7-3-1, Hongo, Bunkyo-ku, Tokyo 113, Japan

(*Received* 7 *December* 1990 *and in final form* 28 *February* 1991)

Abstract—An investigation is carried out on heat transfer by direct contact condensation at a steam–subcooled water interface in a horizontal rectangular channel. Three types of models are used to predict the heat transfer coefficient at the interface. The heat conduction model is used to estimate the lowest limit of heat transfer. The modified k–ε model, which stimulates the near-interface variation of the turbulence quantities, shows the more improved prediction compared with the wall k–ε model and agrees with the experimental results with smooth interfaces. The experimental results with interfacial waves are predicted quantitatively by introducing the interfacial wave effect into the surface renewal model.

1. INTRODUCTION

GAS–LIQUID interfaces appear in many industrial devices, including heat exchangers, which utilize direct contact condensation. Many studies on heat and mass transfer phenomena at the interfaces have been performed. They were reviewed by Bankoff [1] and Sideman and Moalem-Maron [2], and empirical correlations have been proposed [1–4]. There are also studies investigating the turbulent characteristics in the vicinity of gas–liquid interfaces. Turbulent motion transfers heat, mass, and momentum more effectively than molecular motion does. To get a better understanding of turbulent characteristics, a number of experiments [5–9] have been conducted. Komori *et al.* [8] performed an experiment on an open-channel flow and found that the surface renewal eddies were correlated with the bursting phenomena which occurred on the wall. Banerjee [9] performed experiments and computations about the turbulence structure below the sheared smooth air–water interface, and observed the streaky or patchy structure, similar to the wall turbulence, in the vicinity of the smooth interface.

In analyzing turbulent flow, the k–ε model has been developed to simulate the high Reynolds number turbulence and the wall turbulence. The asymptotic variation of the turbulence quantities to the wall was investigated by Patel *et al.* [10]. When the solid wall is replaced by the gas–liquid interface, however, the asymptotic variation of the turbulence quantities to the interface becomes different from that to the solid wall. Therefore, the k–ε model has to be modified to describe the characteristics of the gas–liquid interface. Some attempts [11–13] to solve the flow field below the gas–liquid interface by using the k–ε model have been reported. At present, however, the near-interface characteristics of turbulence is not well understood, because of difficulties of precise measurement.

In this study, heat transfer by direct contact condensation at a steam–subcooled water interface in a horizontal rectangular channel is investigated. Steam and subcooled water flow cocurrently and the flow regimes are the stratified and wavy flows. The heat transfer coefficient at the interface is predicted by three methods—the modified k–ε model, the surface renewal model, and the heat conduction model. The damping factors in the modified k–ε model are adjusted to simulate the near-interface variation of the turbulence quantities. The modified k–ε model is based on the one proposed for the wall turbulence by Myong *et al.* [14]. In performing the numerical analysis using the modified k–ε model, both the steam flow and the water flow are simultaneously computed by the finite difference method. In the prediction by the surface renewal model, three disturbance sources are considered—the bursts from the wall, the bursts at the interface, and the interfacial waves. By estimating the surface renewal rate of each phenomenon, the heat transfer coefficient is calculated. In the heat conduction model, an analytical solution is adopted. This result is used as a fundamental reference in evaluating the results of the other two models. The results predicted by these three models are compared with the experimental results of Lim *et al.* [4] and Murata *et al.* [15].

2. EXPERIMENTS OF LIM *et al.* AND MURATA *et al.*

Lim *et al.* [4] and Murata *et al.* [15] measured the heat transfer coefficient at the steam–subcooled water interface in a horizontal rectangular channel. Steam and water flowed cocurrently, and the flow patterns were stratified and wavy. The dimensions of the test section were 63.5 mm high, 304.8 mm wide and 1601 mm long in the study of Lim *et al.*, and 45 mm high, 200 mm wide and 1000 mm long in the study of

NOMENCLATURE

A_i^+ function in the modified k–ε model
a_0 coefficient in determining a wave velocity
b channel width [m]
C_{PL} specific heat of water [J kg^{-1} K^{-1}]
C_l, $C_{\varepsilon 1}$, $C_{\varepsilon 2}$, C_μ constants in the k–ε model
c_w wave velocity [m s^{-1}]
D hydraulic equivalent diameter [m]
f_2, f_D, f'_D, f_μ damping factors in the k–ε model
G mass velocity [kg m^{-2} s^{-1}]
g acceleration of gravity [m s^{-2}]
H_G specific enthalpy of gas phase [J kg^{-1}]
H_{fg} latent heat of evaporation [J kg^{-1}]
H_w wave height [m]
h heat transfer coefficient [W K^{-1} m^{-2}]
h_L liquid film thickness [m]
k turbulent kinetic energy [m^2 s^{-2}]
k_w wave number, $2\pi/L_w$ [m^{-1}]
L_w wavelength [m]
Nu Nusselt number
Pr Prandtl number
p pressure [Pa]
Re Reynolds number, $U_m D/\nu$
Re_x Reynolds number for the correlations of Lim *et al.*, $U_m x/\nu$
R_t turbulent Reynolds number
s surface renewal rate [s^{-1}]
T temperature [°C]
T_{LM} bulk temperature of liquid phase [°C]
T_b bursting period [s]
T_b^+ non-dimensional bursting period, $u_*^2 T_b/\nu$
t time [s]
U velocity in streamwise direction [m s^{-1}]
U_{CL} critical velocity of the Kelvin–Helmholtz instability [m s^{-1}]
u velocity fluctuation in streamwise direction [m s^{-1}]
u_* friction velocity [m s^{-1}]
V velocity in vertical direction [m s^{-1}]
v velocity fluctuation in vertical direction [m s^{-1}]
W mass flow rate [kg s^{-1}]
W_c mass flow rate of condensate [kg s^{-1}]
x coordinate in streamwise direction [m]
y coordinate in vertical direction [m]
y^+ non-dimensional distance, $u_* y/\nu$
y_i distance from the interface [m].

Greek symbols

α_0, α_1 coefficients
β_1 coefficient
δ_{ij} Kronecker's function: 1 if $i = j$; 0 otherwise
ε dissipation rate [m^2 s^{-3}]
κ thermal diffusivity [m^2 s^{-1}]
λ thermal conductivity [W m^{-1} K^{-1}]
μ viscosity coefficient [Pa s]
ν kinematic viscosity [m^2 s^{-1}]
ν_t eddy viscosity [m^2 s^{-1}]
ρ density [kg m^{-3}]
σ_k, σ_ε, σ_t constants in the k–ε model
σ surface tension [N m^{-1}].

Subscripts

a center-line of single phase flow
b bursts at walls
bi bursts at interfaces
G gas
i interface
in inlet value
L liquid
m averaged value in a cross-section of each phase
S saturation
w wave
x length scale of the distance from the entrance
* friction velocity.

Murata *et al.* They both measured the steam velocity profile in the vertical direction by electrically heated pitot tubes at five locations downstream in the study of Lim *et al.*, and four locations downstream in the study of Murata *et al.* Their experimental conditions are shown in Table 1. In Table 1, the length scales and the velocity scales of Reynolds numbers are the hydraulic equivalent diameters and the mean velocities, respectively. The experiments of Lim *et al.* cover a range of the higher Reynolds number of the steam flow. Lim *et al.* [3] calculated the bulk liquid temperature at the axial distance, x, from the energy balance (see Fig. 1) as

$$T_{LM}(x) = \frac{1}{C_{PL}} \left\{ \frac{W_L(0)\,[C_{PL} T_{LM}(0) - H_G]}{W_L(x)} + H_G \right\}. \quad (1)$$

The local heat transfer coefficient was defined as

$$h(x) = \frac{\mathrm{d}W_c}{\mathrm{d}x} \frac{(H_G - C_{PL} T_S)}{b[T_S - T_{LM}(x)]}. \quad (2)$$

The average heat transfer coefficient was calculated by

$$\bar{h}(x) = \frac{1}{x} \int_0^x h(x)\,\mathrm{d}x = \frac{C_{PL}(H_G - C_{PL} T_S)}{b\beta_1 x} \times \left\langle W_L(x) - W_L(0) + \frac{W_L(0)\alpha_1}{\beta_1} \times \ln \left\{ \frac{W_L(x)\beta_1 - W_L(0)\alpha_1}{C_{PL} W_L(0)\,[T_S - T_{LM}(0)]} \right\} \right\rangle \quad (3)$$

where

$$\alpha_1 = C_{PL} T_{LM}(0) - H_G$$
$$\beta_1 = C_{PL} T_S - H_G.$$

Table 1. The experimental conditions and the computational conditions (Runs 1–3)

	Inlet Reynolds number	Inlet temperature (°C)
Lim *et al.*		
Water	1973–30 200	1, 25, 50
Steam	17 000–65 200	105–140
Murata *et al.*		
Water	6900–21 900	25, 60, 70
Steam	7700–19 700	100
Run 1 (Murata *et al.*)		
Water	21 500	70.0
Steam	7800	100.0
Run 2 (Lim *et al.*)		
Water	13 597	25.3
Steam	28 947	137.7
Run 3 (Lim *et al.*)		
Water	23 414	51.0
Steam	28 327	137.7

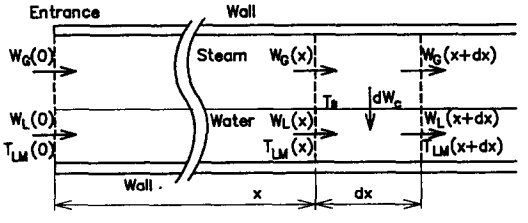

FIG. 1. Model used for the energy balance.

They defined the average non-dimensional numbers as

$$Re_{Lx} = \frac{2xG_L}{\mu_L(0)+\mu_L(x)} \quad (4)$$

$$Re_{Gx} = \frac{xG_G}{\mu_G} \quad (5)$$

$$Nu_x = \frac{2\bar{h}x}{\lambda_L(0)+\lambda_L(x)} \quad (6)$$

where G is the average mass velocity. Lim *et al.* [3] proposed the following two correlations depending upon the shape of the interfaces:

for smooth interfaces

$$Nu_x = 0.534 Re_{Gx}^{0.58} Re_{Lx}^{0.09} Pr_L^{0.3} \quad (7)$$

for wavy interfaces

$$Nu_x = 0.0291 Re_{Gx}^{0.58} Re_{Lx}^{0.42} Pr_L^{0.3}. \quad (8)$$

3. MODELS

3.1. *The modified k–ε model*

The conservation equations of the two-dimensional turbulent flow are

$$\frac{\partial U_j}{\partial x_j} = 0 \quad (9)$$

Table 2. Exponents with respect to the distance from the boundary expressing the near-boundary variation of the turbulence quantities

	Wall side	Interface side	The modified k–ε model
ε	0	0	0
k^2/ε	4	0	0
f_μ	−1	1 (or larger)	1
$-\overline{uv}$	3	1 (or larger)	1
ν_t	3	1 (or larger)	1
$\partial U/\partial y$	0	0	0

$$\frac{DU_i}{Dt} = \frac{\partial}{\partial x_j}\left[(\nu+\nu_t)\frac{\partial U_i}{\partial x_j}\right] - \frac{1}{\rho}\frac{\partial p}{\partial x_i} \quad (i=1,2) \quad (10)$$

$$\frac{DT}{Dt} = \frac{\partial}{\partial x_j}\left[\left(\kappa+\frac{\nu_t}{\sigma_t}\right)\frac{\partial T}{\partial x_j}\right] \quad (11)$$

$$\frac{Dk}{Dt} = \frac{\partial}{\partial x_j}\left[\left(\nu+\frac{\nu_t}{\sigma_k}\right)\frac{\partial k}{\partial x_j}\right] - \overline{u_i u_j}\frac{\partial U_i}{\partial x_j} - \varepsilon \quad (12)$$

$$\frac{D\varepsilon}{Dt} = \frac{\partial}{\partial x_j}\left[\left(\nu+\frac{\nu_t}{\sigma_\varepsilon}\right)\frac{\partial \varepsilon}{\partial x_j}\right] + C_{\varepsilon 1}\frac{\varepsilon}{k}(-\overline{u_i u_j})\frac{\partial U_i}{\partial x_j} - C_{\varepsilon 2} f_2 \frac{\varepsilon^2}{k} \quad (13)$$

where

$$\frac{D}{Dt} = \frac{\partial}{\partial t} + U_j\frac{\partial}{\partial x_j}$$

$$-\overline{u_i u_j} = \nu_t\left(\frac{\partial U_i}{\partial x_j}+\frac{\partial U_j}{\partial x_i}\right) - \frac{2}{3}k\delta_{ij} \quad (14)$$

$$\nu_t = C_\mu f_\mu \frac{k^2}{\varepsilon} \quad (15)$$

$\sigma_k = 1.4$, $\sigma_\varepsilon = 1.3$, $\sigma_t = 0.9$, $C_{\varepsilon 1} = 1.4$, $C_{\varepsilon 2} = 1.8$, $C_\mu = 0.09$.

In the above equations, subscripts i and j are used in accordance with the ordinary tensor expression; 1 means the streamwise direction and 2 the vertical direction.

The k–ε turbulence model of Myong *et al.* is for the wall boundary layer. Their k–ε model has to be modified to stimulate the near-interface characteristics of the turbulence quantities. The turbulence quantities in the layer close to the interface can be examined in the same way as those near the wall [10]. At the interface, the velocity fluctuations parallel to the interface can have a non-zero value. The velocity fluctuation normal to the interface becomes zero at the interface. This means that the turbulent kinetic energy has the non-zero value at the gas–liquid interface. The near-boundary characteristics of turbulence can be approximated by the lowest order term in the Taylor series expansion with respect to the distance from the boundary [10], as shown in Table 2. If the lowest

exponent of the Reynolds stress is assumed to be unity, the eddy viscosity decays more slowly in the vicinity of the interface than in the vicinity of the solid wall. This implies that the turbulent transport is more dominant near the gas–liquid interface than near the wall.

The near-interface variation of the Reynolds stress is represented by the damping factor, f_μ, which describes the boundary-proximity effect in the eddy viscosity. The modified k–ε model is explained briefly below. In the modified k–ε model, the lowest exponent with respect to the distance, y_i, from the interface in the Reynolds stress is assumed to be unity. This near-interface variation is described by choosing the damping factors as [16]

$$f_\mu = \left(1 + \frac{C}{\sqrt{R_t}}\right) f_D \tag{16}$$

$$R_t = \frac{k^2}{\nu\varepsilon}, \quad C_l = 3.45$$

where

$$f_D = [1 - \exp(-y_i^+/A_i^+)] \tag{17}$$

$$A_i^+ = 70\left[1 - \exp\left(-\frac{u_{i*}}{u_*}\right)\right]. \tag{18}$$

In equation (18), A_i^+ is expressed as a function of the friction velocities. The experimental results showed that the wall side turbulence was not affected by the interfacial shear stress [16, 17]. To prevent the interface-proximity effect from affecting the turbulence of the wall side, this dependence on the friction velocities is introduced.

Myong *et al.* [14] expressed the destruction term in the dissipation rate equation with a damping factor as

$$f_2 = \{1 - (2/9)\exp[-(R_t/6)^2]\} f'_D. \tag{19}$$

In the wall turbulence, the destruction term is proportional to y^{-2}, so f'_D is a function proportional to y^2. In the turbulence near the interface, however, k and ε have non-zero finite values at the interface, so there is no restriction for f'_D from the near-interface characteristics. In the modified k–ε model, it is assumed that the factor, f'_D, is not affected by the existence of the interface. The adopted form is the same as that of Myong *et al.*

$$f'_D = [1 - \exp(-y^+/5)]^2. \tag{20}$$

The turbulent kinetic energy, k, has a non-zero finite value at the interface. In estimating this value, the idea of Nezu and Nakagawa [13] is adopted. They connected the turbulent kinetic energy, k_i, at the gas–liquid interface to the turbulent kinetic energy, k_a, at the center-line of the single phase flow between two parallel plates. The relationship between k_i and k_a was expressed as

$$k_i = 0.8k_a \tag{21}$$

$$(k = 0; \text{ at the wall}).$$

They chose 0.8 as the coefficient from the experimental results. In this study, the value, k_a, is approximated as u_*^2 from the numerical results of Kim *et al.* [18].

The boundary condition of the dissipation rate at the gas–liquid interface is determined from the near-interface variation of the turbulent kinetic energy equation of the two-dimensional boundary layer [16]. If the steady and fully developed flow is assumed, the turbulent kinetic energy equation approaches

$$\varepsilon_i = \frac{\partial}{\partial y}\left[\left(\nu + \frac{\nu_t}{\sigma_k}\right)\frac{\partial k}{\partial y}\right]\Bigg|_i \tag{22}$$

$$\left(\varepsilon = \nu\frac{\partial^2 k}{\partial y^2}; \text{ at the wall}\right).$$

Equation (22) is the exact boundary condition of ε at the gas–liquid interface of the steady and fully developed flow. In this study, the flow and thermal fields are not fully developed, so it is assumed that the turbulent kinetic energy at the interface does not change drastically in the streamwise direction.

The modified k–ε model assumes that the interface is smooth. It should be noted that the modified k–ε model is not applicable to the phenomena with interfacial waves.

3.2. *Surface renewal model*

The surface renewal model was originally proposed by Danckwerts [19]. This model assumes that the molecular diffusion is renewed by the surface renewal eddies with the surface renewal rate, s. This model gives the heat transfer coefficient, h, as

$$h = \rho C_{PL}\sqrt{(\kappa s)}. \tag{23}$$

In this study, the surface renewal eddies are assumed to be generated by three disturbance sources—the bursts from the wall, the bursts at the interface, and the interfacial waves. As Komori *et al.* [8] pointed out, the gas–liquid interface of an open-channel flow is strongly affected by the wall bursting phenomenon. When the interfacial shear stress is imposed on the interface, Banerjee [9] showed that the bursting phenomenon occurred just below the interface in the stratified flow (see Fig. 2(a)). Banerjee [9] showed equation (24) could be applied to the bursting phenomenon at the interface by evaluating the friction velocity at the interface, as well as the bursting phenomenon at the wall

$$T_b^+ \equiv \frac{u_*^2}{\nu} T_b = 85. \tag{24}$$

In this study, the bursting periods are estimated by equation (24), where the friction velocity is given by the Blasius equation. The surface renewal rate is a reciprocal of the bursting period.

When interfacial waves are formed at the gas–liquid interface, the increase of heat transfer rates has been

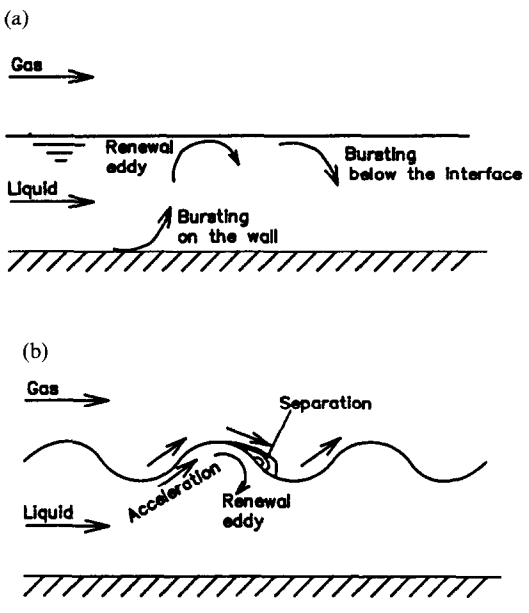

FIG. 2. Conceptual sketch of the surface renewal model: (a) for a smooth interface; (b) for a wavy interface.

reported by Lim *et al.* [3] and Murata *et al.* [15]. This wave effect should be introduced in the surface renewal model. As shown in Fig. 2(b), the windward side of waves is sheared by the gas flow. On the leeward side, the separation of flow occurs, and the interfacial shear stress is smaller than that on the windward side. The accelerated liquid on the windward side goes into the weakly sheared region on the leeward side, and it goes downwards. Okuda *et al.* [20] observed this downward motion. This motion causes eddies which renew the interface. It is assumed that the surface renewal occurs with the frequency of interfacial waves by the downward motion described above. The period of this renewal motion is determined as follows.

The wavelength of the interfacial waves is approximated by the critical wavelength of the Kelvin–Helmholtz instability

$$L_w = 2\pi\sqrt{\left(\frac{\sigma}{(\rho_L-\rho_G)g}\right)}. \tag{25}$$

The wave velocity relative to the bulk water is determined by using the analytical results of finite amplitude waves in deep water [21]

$$c_w = \sqrt{\left(\frac{gL_w}{2\pi}\right)}\left[1+\left(\frac{2\pi a_0}{L_w}\right)^2\right]^{0.5} \tag{26}$$

$$a_0 = \frac{H_w}{2}\left[1-\frac{3\pi^2}{8}\left(\frac{H_w}{L_w}\right)^2\right]. \tag{27}$$

The wave height, H_w, in equation (27) is estimated by using the correlation of Bontozoglou and Hanratty [22]. They proposed the empirical correlation of wave steepness, H_w/L_w, as

$$\frac{H_w}{L_w} = 0.079\alpha_0\frac{U_G-U_L}{U_{CL}} \tag{28}$$

where

$$U_{CL} = \sqrt{\left(\frac{\rho_L+\rho_G}{\rho_L\rho_G}\left[\frac{2\pi\sigma}{L_w}+(\rho_L-\rho_G)\frac{L_w g}{2\pi}\right]\right)}. \tag{29}$$

The value of α_0 in equation (28) is calculated by using the third-order polynomial as

$$\alpha_0 = -0.0744+1.2421(k_w h_L)-0.5015(k_w h_L)^2 +0.0701(k_w h_L)^3. \tag{30}$$

The surface renewal rate by waves, s_w, is determined as

$$s_w = c_w/L_w. \tag{31}$$

The total surface renewal rates of smooth and wavy interfaces are assumed to be expressed as

$$s_{smooth} = s_b+s_{bi} \tag{32}$$

$$s_{wavy} = s_b+s_{bi}+s_w \tag{33}$$

where the subscripts b, bi, and w denote the bursts from the wall, the bursts at the interface, and the interfacial waves, respectively. These values are substituted into s in equation (23) and the heat transfer coefficient is evaluated. The experimental results are used in calculating the surface renewal rates. The average heat transfer coefficient is calculated by averaging the surface renewal rate at each location in the streamwise direction. The estimated surface renewal rates vary from 9.5 to 10.3 Hz for the interfacial wave effect, s_w, from 0.1 to 37.5 Hz for the wall bursting effect, s_b, and from 0.2 to 10.3 Hz for the interfacial bursting effect, s_{bi}. The larger values of s_b and s_{bi} correspond to the higher Reynolds numbers of water and steam, respectively.

3.3. *Heat conduction model*

In the heat conduction model, convective heat transfer is ignored. By this assumption, the energy equation becomes

$$\frac{\partial T_L}{\partial t} = \kappa\frac{\partial^2 T_L}{\partial y_i^2}. \tag{34}$$

For simplicity, the depth of water is assumed to be infinity. The boundary and initial conditions are

$$T_L = T_S\ (y_i = 0;\ \text{at the interface}) \tag{35}$$

$$T_L = \text{a finite value}\ (y_i = \infty;\ \text{at the wall}) \tag{36}$$

$$T_L = T_{Lin}\ (t = 0). \tag{37}$$

The analytical solution of equation (34) is the well-known complementary error function [23]

$$\frac{T_L-T_{Lin}}{T_S-T_{Lin}} = \text{erfc}\left(\frac{y_i}{2\sqrt{(\kappa t)}}\right). \tag{38}$$

Here, time, t, is related to the distance, x, from the entrance as

$$x = U_m t. \tag{39}$$

By substituting equation (39) into equation (38), we obtain

$$\frac{T_L - T_{Lin}}{T_S - T_{Lin}} = \mathrm{erfc}\left(\frac{y_i}{2}\sqrt{\left(\frac{U_m}{\kappa x}\right)}\right). \tag{40}$$

The bulk liquid temperature is calculated by assuming the uniform velocity profile. The heat transfer coefficient and the mass flow rate of condensate are calculated from the energy balance equations (1)–(3). The results are arranged in the same way as explained in Section 2.

4. NUMERICAL PROCEDURES

The two-dimensional finite difference method is employed for the numerical analysis of the modified k–ε model. The SIMPLER algorithm by Patankar [24] is used. Both the steam and water flows are solved by making the interfacial shear stress and the vertical mass flow rate coincide at the interface. Because the phenomenon is steady, the differential term with respect to time is utilized as the inertia term in computations. Properties are interpolated from a property table at each grid point as temperature-dependent functions. The following items are assumed in performing the numerical analysis:

(1) Flow is two-dimensional.
(2) No-slip at walls.
(3) Walls are thermally insulated.
(4) Water level is uniform.
(5) Inlet water temperature is uniform.

The three cases, Runs 1, 2 and 3 in Table 1, are selected for the reference of the computation by the modified k–ε model, because the steam flow rate is low and the water level does not change drastically in the streamwise direction. Run 1 is chosen as a smooth interface result from Murata *et al.* and Runs 2 and 3 as wavy interface results from Lim *et al.* The depth of each layer is given by the experiments as 13.0 mm for the water layer and 32.0 mm for the steam layer in Run 1, and 15.83 mm for the water layer and 47.67 mm for the steam layer in Runs 2 and 3. In the streamwise direction, computational length is 0.6 m from the entrance. At the interface, the coincidence of streamwise velocities and the interfacial shear stresses of both phases are satisfied. The boundary condition of the vertical steam velocity at the interface is determined from the energy balance equation

$$\frac{\mathrm{d}(C_{PL} W_L(x) T_{LM}(x))}{\mathrm{d}x} = -\rho_G V_{iG}(H_{fg} + T_S C_{PL}). \tag{41}$$

The vertical velocity of water at the interface is calculated from the vertical steam velocity determined by equation (41) to conserve the mass across the interface.

Judging from the velocity scales of both phases, the interface on the gas phase side can be treated as a solid wall. The fully developed profiles are given as the inlet boundary conditions. The grid points are so densely distributed in the vicinity of the wall and the interface as shown by a tangent hyperbolic function. In the vertical direction, 52 grid points for the water layer and 32 grid points for the steam layer are adopted. In the streamwise direction, there are 12 grid points for each phase. The grid number was sufficient to obtain a grid-independent solution. The convergence is judged to be enough when the mass conservation error becomes within 0.5%. The computations were carried out on a super-computer HITAC S-820 at the University of Tokyo.

5. RESULTS AND DISCUSSION

The experimental results of Lim *et al.* [4] and Murata *et al.* [15] are shown in Fig. 3. The data of Lim *et al.* agree very well with the correlation (equation (8)) for wavy interfaces, when Re_{Lx} is large. There are less data for smooth interfaces and they scatter. The experimental conditions of Murata *et al.* cover the low Reynolds number region of the steam flow and their data are located around the correlation (equation (7)) for smooth interfaces.

The results of the wall k–ε model of Myong *et al.* [14] are also presented for comparison. The results of the modified k–ε model and the wall k–ε model are displayed by solid and broken lines in Figs. 4–6. Figure 4 shows the predicted results for a smooth interface. The wall k–ε model predicts the intermediate values between the correlation (equation (7)) for the smooth interface by Lim *et al.* and the results by the heat conduction model. The heat conduction model can be regarded as the lowest limit of heat transfer, because it includes neither laminar convective transport nor turbulent transport. The modified k–ε model

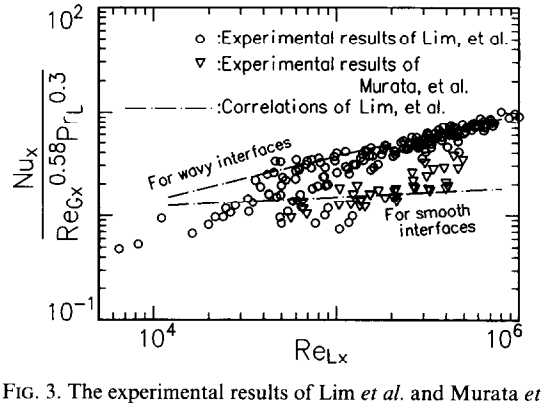

FIG. 3. The experimental results of Lim *et al.* and Murata *et al.* with the correlations of Lim *et al.*

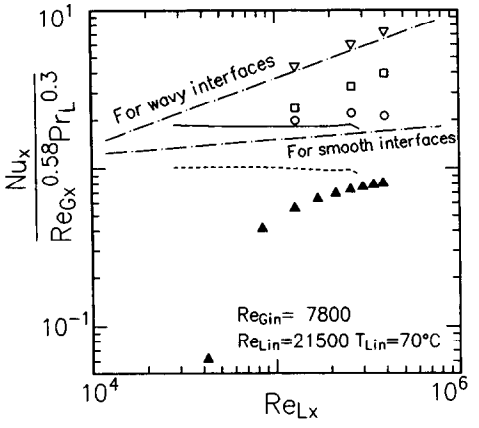

FIG. 4. The predicted heat transfer by three models expressed in the coordinates of Lim *et al.*; the case for a smooth interface of Murata *et al.* (Run 1). The marks and line types represent: (○) the experimental results; (□) the surface renewal model (without wave effect); (▽) the surface renewal model (with wave effect); (▲) the heat conduction model; (———) the modified k–ε model; (----) the wall k–ε model; (— · — · —) the correlations of Lim *et al.*

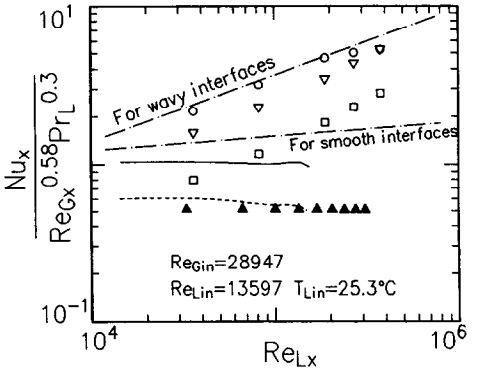

FIG. 5. The predicted heat transfer by three models expressed in the coordinates of Lim *et al.*; the case for a wavy interface of Lim *et al.* (Run 2). The marks and line types are the same as those in Fig. 4.

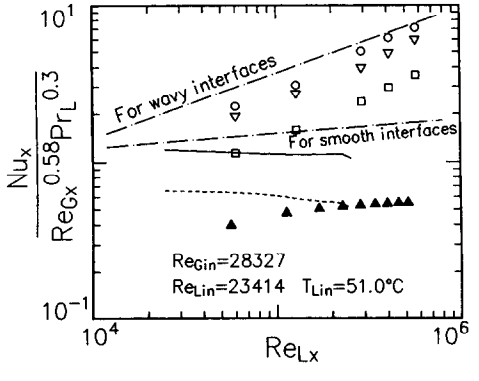

FIG. 6. The predicted heat transfer by three models expressed in the coordinates of Lim *et al.*; the case for a wavy interface of Lim *et al.* (Run 3). The marks and line types are the same as those in Fig. 4.

predicts the value closer to both the experimental results and the correlation of Lim *et al.* for smooth interfaces compared with the result of the wall k–ε model. The surface renewal model excluding interfacial waves gives a little larger values than the experimental results and the modified k–ε model.

In the cases of wavy interfaces in Figs. 5 and 6, the modified k–ε model predicts smaller heat transfer rates than the correlation of Lim *et al.* for smooth interfaces. But the improvement is clearly seen when compared with the results of the wall k–ε model. The experimental results show larger values than the results of the modified k–ε model. As mentioned in Section 3.1, the modified k–ε model is not applicable to the case with interfacial waves.

In Figs. 5 and 6, the predicted data series of the surface renewal model excluding the interfacial wave effect cross the correlation for smooth interfaces, and are close to those of the modified k–ε model. The comparison with the experimental results shows a discrepancy. By introducing the wave effect, however, the results of the surface renewal model become closer to the experimental data.

In the modified k–ε model, the turbulent transport is described by averaged values. On the contrary, it is done in a dynamical way in the surface renewal model. It is interesting that the modified k–ε model and the surface renewal model excluding wave effect give similar results.

The results of the surface renewal model excluding wave effect are shown in Fig. 7. In this case, all the experimental conditions of Lim *et al.* are used with equation (32). The predicted data fall on a straight line very well. The data for higher Reynolds numbers of the liquid flow show higher values than the correlation for smooth interfaces. In the surface renewal model, it is assumed that all the bursts on the wall reach the interface. However, Komori *et al.* [8] measured that only 90% of the wall bursts arrived at the interface in their experimental range. When the liquid flow Reynolds number becomes larger, the non-dimensional distance, y^+, from the wall to the inter-

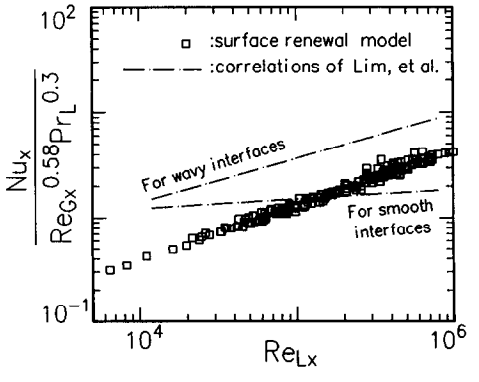

FIG. 7. The predicted heat transfer by the surface renewal model excluding wave effect expressed in the coordinates of Lim *et al.*

face becomes larger. Thus, the arrival rate of the wall bursts to the interface may decrease. The surface renewal model will be refined by experimental results covering the higher Reynolds number range of the liquid flow.

The experimental results which are located above the center of two correlations in Fig. 3 are regarded as the wavy cases in this study. The results of the surface renewal model with wave effect lie between two correlations (equations (7) and (8)) as shown in Fig. 8. As Lim *et al.* showed in their paper, the range of their experiments extends to higher steam velocities. They observed roll waves for some cases, which could promote heat transfer. The roll waves and the finite amplitude waves used in the present surface renewal model have quite different characteristics. This difference can be one of the reasons for the discrepancy seen in Fig. 8. The approximate way to estimate the wave characteristics and the arrival rate of the wall bursts to the interface might be major reasons for discrepancy.

6. CONCLUDING REMARKS

The heat transfer coefficient by direct contact condensation at a steam–subcooled water interface was predicted by using three types of models.

The modified k–ε model, which simulates the near-interface variation of the turbulence quantities, showed the better agreement with the experimental results in predicting the heat transfer at the interface compared with the wall k–ε model. The modified k–ε model predicted the heat transfer coefficient close to that of the experiments for a smooth interface and the correlation of Lim *et al.* for smooth interfaces. On the other hand, the wall k–ε model predicted lower values close to the results of the heat conduction model, which is considered to give the lowest limit of heat transfer at the interface.

The surface renewal model excluding wave effect predicted a value close to both the modified k–ε model and the correlation for smooth interfaces, equation (7). The experimental results with interfacial waves were predicted by introducing the wave effect into the surface renewal model. This indicates the validity of the method to estimate the surface renewal rate. The concept that the surface renewal eddies are caused by the wall bursts, the interfacial bursts, and the interfacial waves, seems to be valid.

The modified k–ε model and the surface renewal model have different ideas in predicting the heat transfer. In other words, these two models describe the same phenomenon from different standpoints. It is interesting that the results showed heat transfer rates close to each other so long as smooth interfaces are considered.

For further refinement of the models, information on the near-interface characteristics of turbulence for a wider range of Reynolds numbers and the characteristics of wind-induced waves are required.

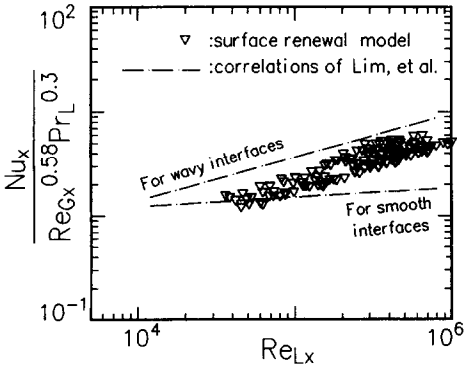

FIG. 8. The predicted heat transfer by the surface renewal model with wave effect expressed in the coordinates of Lim *et al.*

REFERENCES

1. S. G. Bankoff, Some condensation studies pertinent to LWR safety, *Int. J. Multiphase Flow* **6,** 51–67 (1980).
2. S. Sideman and D. Moalem-Maron, Direct contact condensation, *Advances in Heat Transfer*, Vol. 15, pp. 227–281. Academic Press, New York (1982).
3. I. S. Lim, R. S. Tankin and M. C. Yuen, Condensation measurement of horizontal cocurrent steam/water flow, *Trans. ASME J. Heat Transfer* **106,** 425–432 (1984).
4. I. S. Lim, S. G. Bankoff, R. S. Tankin and M. C. Yuen, Cocurrent steam/water flow in a horizontal channel, NUREG/CR-2289 (1981).
5. T. K. Cheung and R. L. Street, The turbulent layer in the water at an air water interface, *J. Fluid Mech.* **194,** 133–151 (1988).
6. I. Nezu and W. Rodi, Open-channel flow measurements with a laser Doppler anemometer, *J. Hydraulic Engng* **112,** 335–355 (1986).
7. H. Nakagawa and I. Nezu, Structure of space–time correlations of bursting phenomena in an open-channel flow, *J. Fluid Mech.* **104,** 1–43 (1981).
8. S. Komori, Y. Murakami and H. Ueda, The relationship between surface-renewal and bursting motions in an open-channel flow, *J. Fluid Mech.* **203,** 103–123 (1989).
9. S. Banerjee, Turbulence structure and transport mechanisms at interfaces, *Proc. 9th Int. Heat Transfer Conf.*, Jerusalem, Israel, Vol. 1, pp. 395–418 (1990).
10. V. C. Patel, W. Rodi and G. Scheuerer, Turbulence models for near-wall and low Reynolds number flows: a review, *AIAA J.* **23,** 1308–1319 (1985).
11. M. Akai, A. Inoue and S. Aoki, The prediction of stratified two-phase flow with a two-equation model of turbulence, *Int. J. Multiphase Flow* **7,** 21–39 (1981).
12. I. Celic and W. Rodi, Simulation of free-surface effects in turbulent channel flows, *PhysicoChem. Hydrodyn.* **5,** 217–227 (1984).
13. I. Nezu and H. Nakagawa, Numerical calculation of turbulent open-channel flows by using a modified k–ε turbulence model, *Trans. Jpn. Soc. Civil Engng* **387,** 125–134 (1987) (in Japanese).
14. H. K. Myong, N. Kasagi and M. Hirata, Numerical prediction of turbulent pipe flow heat transfer for various Prandtl number fluids with the improved k–ε turbulence model, *JSME Int. J.* **32,** 613–622 (1989).
15. A. Murata, E. Hihara and T. Saito, Heat transfer with

condensation at a steam–water interface in a horizontal channel, *Trans. Jpn. Soc. Mech. Engng* **57**(536B), 1385–1389 (1991) (in Japanese).
16. A. Murata, E. Hihara and T. Saito, Turbulence below an air–water interface in a horizontal channel, *Turbulence modification in multiphase flows, 1st Joint ASME–JSME Fluids Engng Conf.* (Edited by E. E. Michaelides, T. Fulcano and A. Serizawa), Portland, U.S.A., FED-Vol. 110, 67–74 (1991).
17. M. Rashidi and S. Banerjee, The effect of boundary conditions and shear rate on streak formation and breakdown in turbulent channel flows, *Physics Fluids* **A2,** 1827–1838 (1990).
18. J. Kim, P. Moin and R. Moser, Turbulence statistics in fully developed channel flow at low Reynolds number, *J. Fluid Mech.* **177,** 133–166 (1987).
19. P. V. Danckwerts, Significance of liquid-film coefficients in gas absorption, *Ind. Engng Chem.* **43,** 1460–1467 (1951).
20. K. Okuda, S. Kawai and Y. Toba, Measurement of skin friction distribution along the surface of wind waves, *J. Oceanograph. Soc. Jpn.* **33,** 190–198 (1977).
21. L. Skjelbreia, *Stokes' Third Order Approximation, Tables of Function.* Council on Wave Research, The Engineering Foundation (1958).
22. V. Bontozoglou and T. J. Hanratty, Wave height estimation in stratified gas–liquid flows, *A.I.Ch.E. Jl* **35,** 1346–1350 (1989).
23. T. K. Sherwood, R. L. Pigford and C. R. Wilke, *Mass Transfer*, p. 70. McGraw-Hill, New York (1975).
24. S. V. Patankar, *Numerical Heat Transfer and Fluid Flow.* Hemisphere, New York (1980).

PREDICTION DU TRANSFERT THERMIQUE LORS DE LA CONDENSATION PAR CONTACT DIRECT A L'INTERFACE VAPEUR–EAU SOUS REFROIDIE

Résumé—On étudie le transfert thermique lors de la condensation par contact direct à l'interface de la vapeur avec l'eau sous-refroidie dans un canal horizontal rectangulaire. Trois types de modèles sont utilisés pour prédire le coefficient de transfert thermique à l'interface. Le modèle de conduction estime la limite inférieure du transfert thermique. Le modèle k–ε qui simule la variation des grandeurs turbulentes près de l'interface, donne l'estimation la plus forte par rapport à celle du modèle k–ε à la paroi et il s'accorde avec les résultats expérimentaux pour dcs interfaces lisses. Les résultats expérimentaux avec des rides interfaciales sont prédits quantitativement en introduisant l'effet de la ride dans le modèle de renouvellement de surface.

BERECHNUNG DES WÄRMEÜBERGANGS BEI DER DIREKTKONDENSATION AN DER GRENZFLÄCHE ZWISCHEN DAMPF UND UNTERKÜHLTEM WASSER

Zusammenfassung—Die Untersuchung beschäftigt sich mit dem Wärmeübergang bei der Direktkondensation an der Grenzfläche zwischen Dampf und unterkühltem Wasser in einem waagerechten rechteckigen Kanal. Es werden drei unterschiedliche Modelle zur Berechnung des Wärmeübergangskoeffizienten an der Grenzfläche benutzt. Das Wärmeleitungsmodell dient zur Abschätzung einer unteren Grenze für den Wärmeübergang. Das modifizierte k–ε Modell, das die Veränderung der turbulenten Größen in der Nähe der Grenzflächen wiedergibt, ermöglicht im Vergleich zum k–ε Modell an der Wand eine verbesserte Berechnung und stimmt gut mit den experimentellen Ergebnissen bei glatter Grenzfläche überein. Die Versuchsergebnisse mit Oberflächenwellen können quantitativ berechnet werden, wenn der Einfluß der Wellen in das Oberflächenerneuerungsmodell eingeführt wird.

ОПРЕДЕЛЕНИЕ ТЕПЛОПЕРЕНОСА ПРИ КОНТАКТНОЙ КОНДЕНСАЦИИ НА ГРАНИЦЕ РАЗДЕЛА ВОДЯНОЙ ПАР–НЕДОГРЕТАЯ ВОДА

Аннотация—Исследуется теплоперенос при контактой конденсации на границе раздела водяной пар–недогретая вода в горизонтальном канале прямоугольного сечения. Для определения коэффициента теплопереноса на границе раздела используются три вида моделей. Модель теплопроводности применяется для оценки нижнего предела передачи тепла. Модифицированная модель k–ε, описывающая изменение величин турбулентности вблизи границы раздела, дает более точные результаты по оравнению с пристенной k–ε моделью и хорошо согласуется с экспериментальными данными для гладких границ раздела. Экспериментальные данные для случая возникновения волн на границе раздела определяются количественно посредством введения эффекта волн на границе раздела в модель обновления поверхности.